

Formation of Host-Guest Complexes on Gold Surface Investigated by Surface-Enhanced IR Absorption Spectroscopy

Yoshiya Inokuchi,^{‡,*} Takahiro Mizuuchi,[‡] Takayuki Ebata,[‡] Toshiaki Ikeda,[‡]

Takeharu Haino,[‡] Tetsunari Kimura,[†] Hao Guo,[†] and Yuji Furutani[†]

Department of Chemistry, Graduate School of Science, Hiroshima University,
Higashi-Hiroshima, Hiroshima 739-8526, Japan, and Institute for Molecular Science,
Myodaiji, Okazaki 444-8585, Japan

*To whom correspondence should be addressed.

E-mail: y-inokuchi@hiroshima-u.ac.jp

Tel: +81-82-424-7101

[‡]Hiroshima University

[†]Institute for Molecular Science

Abstract

We apply surface-enhanced infrared absorption (SEIRA) spectroscopy to host-guest complexes in liquid phase to examine the structural change in the complex formation. Two thiol derivatives of 18-crown-6 (18C6) are chemisorbed on a gold surface, and aqueous solutions of MCl salts (M = Li, Na, K, Rb, and Cs) are put to form $M^+ \cdot 18C6$ complexes. Infrared spectra of these complexes in the 900–2000 cm^{-1} region are obtained by SEIRA spectroscopy. The observed IR spectra show noticeable peaks due to the complex formation, demonstrating that SEIRA spectroscopy will be a powerful method to investigate the structure of host-guest complexes in supramolecular chemistry.

Keywords: water, crown ether, infrared, solvent effect, SEIRA , FTIR, ATR

Introduction

Ionophores capture guest ions selectively and carry them across interfaces efficiently. For instance, 18-crown-6 (18C6) selectively holds K^+ ion among the alkali metal ions dissolved in aqueous phase.^{1,2} The ion selectivity of ionophores has been explained mainly in terms of their size matching with guest ions based on X-ray diffraction analysis.^{1,3} In crystals, however, counter ions are also bonded to guest ions, which substantially affects the complex structure, and the solvent effect on the encapsulation remains to be elucidated because few solvent molecules are included in one unit cell of crystals. Studies on mass, UV, and IR spectroscopy of host-guest complexes as well as theoretical ones have been suggested that the solvent effect is highly involved in the ion selectivity in liquid phase.^{1,2,4-14} Hence, it is necessary to determine the complex structure in solutions at the molecular level in order to reveal the role of the solvent effect in the ion selectivity. Many efforts have been devoted to examining the complex structure in solutions using NMR and EXAFS spectroscopy.^{15,16} These studies have provided a part of structural information of the complexes such as the distance between host species and guest ions and local conformations of host cavities.

In this Letter, we introduce a new approach to the structure of host-guest complexes in supramolecular chemistry by surface-enhanced infrared absorption (SEIRA) spectroscopy, which was used to study the ion transferring process at ion channels of bio systems.^{17,18} Our idea in this study is to synthesize thiol derivatives of ionophores, adsorb them on gold surfaces through S–Au chemical bonds, put solutions of guest ions on them, and measure IR spectra of host-guest complexes by SEIRA spectroscopy. It is possible to observe their IR spectra with high sensitivity, because

gold surfaces strongly enhance the IR absorption of species bound to them.¹⁹ In addition, since ionophores are chemically bonded on gold surfaces and are not easily removed by washing them with solvents, we can use the same surface repeatedly with different guest solutions. In order to demonstrate the capability of this method, we use two thiol compounds of 18C6 and aqueous solutions of alkali metal salts and measure IR spectra of $M^+ \cdot 18C6$ ($M = Li, Na, K, Rb, \text{ and } Cs$) complexes tagged on gold surfaces through hydrocarbon chains. From the IR spectra, we examine the structural change occurring in the encapsulation of the M^+ ions by the 18C6 component. The amplitude of the IR absorption change induced by the complex formation is dependent on the concentration of the M^+ ions in the aqueous solutions, which provides equilibrium constants for the complex formation and describes the interaction between the ion complexes formed on gold surfaces. A few groups have reported the modification of gold nanoparticles with crown ethers.²⁰⁻²³ However, the main purposes of these studies were to evaluate and improve the functionality of the modified particles as ion sensing devices.

Experimental and Computational Methods

Chemicals. All chemicals for synthesis are purchased and used without further treatment. The synthesis of 2-(6-mercaptohexyloxy)methyl-18-crown-6 (**1**) and 2-(mercaptomethyl)-18-crown-6 (**2**) (Figs. 1a and 1b) is carried out by following the procedures described in a paper of Flink et al.²² Hereafter these molecules are called 18C6-C₁OC₆-SH and 18C6-C₁-SH, respectively. The chloride salts of the alkali metals are purchased from Wako Pure Chemicals Industries and are dissolved into high-purity water (Millipore) to prepare aqueous solutions of the alkali metal ions.

SEIRA Spectroscopy. We perform SEIRA spectroscopy of crown ethers tagged on gold surfaces by using a home-made vacuum deposition system and a FTIR spectrometer (Vertex 70, Bruker) coupled with a single reflection Si attenuated total reflection (ATR) system (VeeMAX II, PIKE Technologies). The details of the preparation of gold surfaces on a Si prism have been described in a previous study of Guo et al.²⁴ Briefly, gold surfaces are formed on an unheated Si crystal by thermal deposition of a gold wire from a tungsten basket in a vacuum chamber with a deposition rate of ~ 0.005 nm/s. The thickness of the gold surface is ~ 7 nm, with which the enhancement of IR absorption will be optimum and the distortion of IR spectral features will be minimized.²⁴ A home-made Teflon chamber is mounted on top of the Si crystal to introduce and keep liquid samples on the gold surface. Modification of the gold surface with crown ether (1) or (2) is performed with monitoring IR absorption of the crown ethers. A solution of (1) or (2) dissolved in dimethylsulfoxide (DMSO) with a concentration of $\sim 5 \cdot 10^{-3}$ M is introduced on the gold surface. Crown ethers (1) and (2) are tagged on the gold surface by forming Au-S chemical bonds. We leave the solution of the crown ethers on the gold surface for 30 minutes for achieving complete coverage of the gold surface with the crown ethers. After removing the DMSO solution and washing the surface several times with pure water, the FTIR difference spectra are measured repeatedly with the aqueous solutions of the alkali metal chloride salts and pure water with a 4 cm^{-1} spectral resolution at room temperature. In every exchange process of the metal ions on the same gold surface, we confirm the removal of the metal ions from the gold surface by observing complete disappearance of the IR bands due to the $M^+ \cdot 18C6$ complexes. We also observe IR difference spectra of the $K^+ \cdot 18C6-C_1OC_6$ complex by using KBr solutions. The IR spectra are almost the same

as those with KCl solutions, indicating that counter anions do not involve in the formation of the ion complexes.

Computational. We calculate the structure and IR spectra of the metal ion complexes using crown ethers simplified by terminating the end of the hydrocarbon chain with a CH₃ group. The initial conformational search is performed for the K⁺•18C6-C₁OC₆-CH₃ and bare 18C6-C₁OC₆-CH₃ by using the mixed torsional search with low-mode sampling and the AMBER* force field as implemented in MacroModel V. 9.1.²⁵ Minimum-energy conformers found with the force field calculations are then optimized at the M05-2X/6-31+G(d) level with the polarizable continuum model (PCM) of water using the GAUSSIAN09 program package.²⁶ For the Na⁺, Rb⁺, and Cs⁺ complexes, initial forms for the geometry optimization are produced on the basis of stable conformers of the K⁺•18C6-C₁OC₆-CH₃ complex. Vibrational analysis is carried out for the optimized structures at the same computational levels. Calculated frequencies at the M05-2X/6-31+G(d) level are scaled with a factor of 0.9389 for comparison with the observed IR spectra.

Results and Discussion

Figure 2a shows the IR difference spectrum of 18C6-C₁OC₆ tagged on a gold surface with an aqueous solution of KCl (0.1 M). This spectrum is obtained by subtracting the IR spectrum with pure water from the one with the aqueous solution of KCl. The IR spectrum of 18C6-C₁OC₆-SH (Fig. 2b) is measured by putting pure 18C6-C₁OC₆-SH directly on an unmodified ATR crystal. The gain and depletion signals in Fig. 2a indicate the formation of the K⁺•18C6-C₁OC₆ complex and the

elimination of bare 18C6-C₁OC₆ on the gold surface, respectively. These signals emerge at positions where 18C6-C₁OC₆-SH has IR absorption, as shown with dotted lines in Fig. 2. The vibrational analysis by quantum chemical calculations demonstrates that the IR bands of 18C6-C₁OC₆-SH around 1457, 1352, 1248, 1107, and 950 cm⁻¹ are assigned to the CH₂ bending, CH₂ wagging, CH₂ twisting, C–O stretching, and C–C stretching vibrations, respectively. The strongest signals in the IR difference spectrum are seen around 1100 cm⁻¹ with a minimum at 1119 cm⁻¹ and a maximum at 1098 cm⁻¹. This zigzag band shape suggests that the formation of the K⁺•18C6-C₁OC₆ complex shifts the C–O stretching vibrations to lower frequency. The IR spectra of 18C6-C₁ on the gold surface with an aqueous solution of KCl (0.1 M) and pure 18C6-C₁-SH are displayed in Figs. 2c and 2d, respectively. The IR difference spectrum of K⁺•18C6-C₁ in Fig. 2c is similar to that of K⁺•18C6-C₁OC₆ in Fig. 2a, suggesting that the IR signals in Figs. 2a and 2c are attributed mainly to the 18C6 part.

Figure 3 displays the IR difference spectra of M⁺•18C6-C₁OC₆ tagged on the gold surface with aqueous solutions of MCl (M = Li, Na, K, Rb, and Cs). The concentration of MCl in water ranges from 10⁻⁶ to 2 M, and the dotted (blue) curve in each panel of Fig. 3 corresponds to the spectrum with 2 M. Broad signals around 1650 cm⁻¹ appearing under higher concentrations are due to the bending vibration of H₂O; introduction of MCl to water deforms the structure of liquid water, providing the signal in the difference spectra. In the IR difference spectra of Li⁺ ion (Fig. 3a), the amplitude of signals is quite weaker than that of the other ions, indicating that the encapsulation of Li⁺ ion with 18C6 does not occur on the gold surface. The IR difference spectra of the K⁺, Rb⁺, and Cs⁺ complexes are similar to each other around the C–O stretching vibrations, with a sharp depletion at ~1118 cm⁻¹ and a sharp gain at

$\sim 1097\text{ cm}^{-1}$. These results suggest that the 18C6 part has a similar structure in the K^+ , Rb^+ , and Cs^+ complexes.

In order to obtain the structure of the ion–crown ether complexes and simulate IR difference spectra, we carry out the geometry optimization and vibrational analysis by using 18C6- $\text{C}_1\text{OC}_6\text{-CH}_3$. Figures 4a and 4b are the calculated IR spectra of the $\text{K}^+\cdot 18\text{C6-C}_1\text{OC}_6\text{-CH}_3$ complex and bare 18C6- $\text{C}_1\text{OC}_6\text{-CH}_3$ in water. The solid curves in Figs. 4a and 4b are simulated IR spectra produced by providing each vibration with a Lorentzian component with a full width at half maximum (FWHM) of 10 cm^{-1} . A scaling factor of 0.9389 is employed for the calculated frequencies. The IR spectrum of bare 18C6- $\text{C}_1\text{OC}_6\text{-CH}_3$ (Fig. 4b) has a maximum of the C–O stretching vibrations at 1114 cm^{-1} , and it shifts to lower frequency, 1101 cm^{-1} , with K^+ ion (Fig. 4a). Figure 4c displays the IR difference spectrum between the simulated spectra in Figs. 4a and 4b, giving a maximum at 1096 cm^{-1} and a minimum at 1114 cm^{-1} . This simulated spectrum well reproduces the spectral features of the observed one (Fig. 4d) with a gain and depletion signal around 1100 cm^{-1} . The structure of the K^+ complex and bare one of 18C6- $\text{C}_1\text{OC}_6\text{-CH}_3$ is shown in Figs. 5c and 5a, respectively. In the K^+ complex, the 18C6 part opens its cavity the most, and the K^+ ion is located at the center of the cavity. In addition, the oxygen atom in the chain is also bonded on top of the K^+ ion. As a result, the $\text{K}^+\cdot 18\text{C6-C}_1\text{OC}_6\text{-CH}_3$ complex is folded, and the $\text{K}^+\cdot 18\text{C6}$ part is located close to the hydrocarbon chain. The structure of the Na^+ , Rb^+ , and Cs^+ complexes are also displayed in Fig. 5. The numbers in Fig. 5 are the distance (\AA) between the metal ions and the oxygen atoms. For the K^+ , Rb^+ , and Cs^+ complexes, all the oxygen atoms have similar distances; the average values are 2.82, 2.97, and 3.11 \AA , respectively. In the Rb^+ and Cs^+ complexes, the metal ions are too large to be surrounded completely by the crown cavity and the chains. In the Na^+ complex, two of the seven oxygen atoms

have larger Na⁺•••O distances (2.95 and 2.98 Å) than that of the other five atoms (< 2.8 Å). In the IR difference spectra of the Na⁺•18C6-C₁OC₆ complex (Fig. 3b), another maximum can be seen at 1049 cm⁻¹ in the C–O stretch region, as shown with an arrow. The multiple peaks of the Na⁺ complex may probably reflect the multiple strengths of the Na⁺•••O interactions.

In solutions, the ion encapsulation process of crown ethers will occur independently for each molecule or ion. In contrast, since the crown ethers in our experiment are chemically bonded on the gold surface and are located close to each other, it would be probable that they show cooperative behavior in the encapsulation process. We can obtain information on the cooperativity from the concentration dependence of the FTIR signals, as shown in Fig. 6. The circles in Fig. 6 show the peak-to-peak amplitude of the negative and positive signals around 1100 cm⁻¹ as a function of the concentration of the metal ions. The data are reproduced by Hill equations (solid curves), and the apparent dissociation constant (K_D) and the Hill coefficients are obtained from the fitting.¹⁸ The concentration range from 10⁻⁶ to 2 M cannot cover the whole rise of the dependence curves for all the ion complexes. However, these curves show noticeable difference between the metal ions. The reciprocal of K_D and the Hill coefficients are plotted in Fig. 7 (red open circles). The reciprocal of K_D shows the maximum for K⁺ ion; it is more than one order of magnitude larger than those of the Na⁺, Rb⁺, and Cs⁺ complexes, indicating the selective encapsulation of K⁺ ion by 18C6 over the other ions. All the Hill coefficients are smaller than 1, which suggests a negative cooperativity that the ion complexes on the gold surface inhibit successive formation of ion complexes. In addition, the Hill coefficients are smaller with decreasing the ion size. This means that the complexes of

smaller ions suppress the complex formation more strongly due to higher charge density.

We perform the same experiment also for 18C6-C₁; the IR difference spectra and the dependence of the FTIR signal around 1100 cm⁻¹ on the M⁺ concentration are shown in Figs. 1S and 2S of the Supplementary Information. The IR difference spectra of M⁺•18C6-C₁ are similar to the corresponding ones of M⁺•18C6-C₁OC₆. However, the dependence of the FTIR signal amplitude on the M⁺ concentration (Fig. 2S) is quite different from that of M⁺•18C6-C₁OC₆. The rise of the signal of M⁺•18C6-C₁ is much slower than that of M⁺•18C6-C₁OC₆. The reciprocal of K_D and the Hill coefficients for M⁺•18C6-C₁ are also shown in Fig. 7 (blue closed circles). As seen in Fig. 7a, the selectivity of K⁺ ion is not so obvious for 18C6-C₁ than 18C6-C₁OC₆. The Hill coefficients of the M⁺•18C6-C₁ complexes are evidently smaller than those of M⁺•18C6-C₁OC₆. This suggests that the successive complex formation is more strongly suppressed for M⁺•18C6-C₁ than M⁺•18C6-C₁OC₆. These results can be explained by the complex structure characteristic of the M⁺•18C6-C₁OC₆ complexes. As seen in Fig. 5, the M⁺•18C6-C₁OC₆ complexes are folded because of the ether oxygen atom in the chain. All the oxygen atoms are bonded to the metal ions and the hydrocarbons of the ion complexes face outwardly, making the ion complexes more hydrophobic than the bare form. As a result, the M⁺•18C6 part can sink between the 18C6-C₁OC₆ molecules attached on the gold surface; this can be recognized as the dissolution of the M⁺•18C6 complexes into the hydrophobic phase formed with the 18C6-C₁OC₆ molecules. This dissolution process keeps the M⁺•18C6 parts away from the aqueous solutions and enhances the selectivity of K⁺ ion by the 18C6 part. In contrast, the M⁺•18C6 parts of the M⁺•18C6-C₁ complexes have direct contact to the aqueous solutions even after the complex formation, because the chain is much shorter

and there is no hydrophobic phase in which the $M^+ \cdot 18C6$ part can be dissolved. The metal ions encapsulated by 18C6 are easy to be released into water, and the ion selectivity inherent to 18C6 does not emerge apparently. Since the ion complexes exist at the interface between the 18C6- C_1 layer and aqueous solution, they avoid free metal ions in the aqueous solutions from being close to 18C6- C_1 and encapsulated by 18C6.

Conclusions

In this study, two thiol derivatives of 18C6 [2-(6-mercaptohexyloxy)methyl-18-crown-6 (18C6- C_1OC_6-SH) and 2-(mercaptomethyl)-18-crown-6 (18C6- C_1-SH), Figs. 1a and 1b] were synthesized and adsorbed on gold surfaces through S–Au bonds. The IR difference spectra of the $M^+ \cdot 18C6-C_1OC_6$ and $M^+ \cdot 18C6-C_1$ complexes were observed by surface-enhanced infrared absorption (SEIRA) spectroscopy. The IR spectra in the 900–2000 cm^{-1} region show noticeable peaks due to the structural change in the complex formation. This suggests that SEIRA spectroscopy will be a powerful method to examine the structure of host-guest complexes and the solvent effect on them in solutions.

Acknowledgments

YI thanks the support from the Institute for Molecular Science through the Joint Studies Program (2012-2013).

Supplementary Information Available: The IR difference spectra of the $M^+ \cdot 18C6-C_1$ complexes on the gold surface (Fig. 1S), the concentration dependence of the peak-to-peak intensity around 1100 cm^{-1} in the IR difference spectra of the $M^+ \cdot 18C6-C_1$ complexes (Fig. 2S).

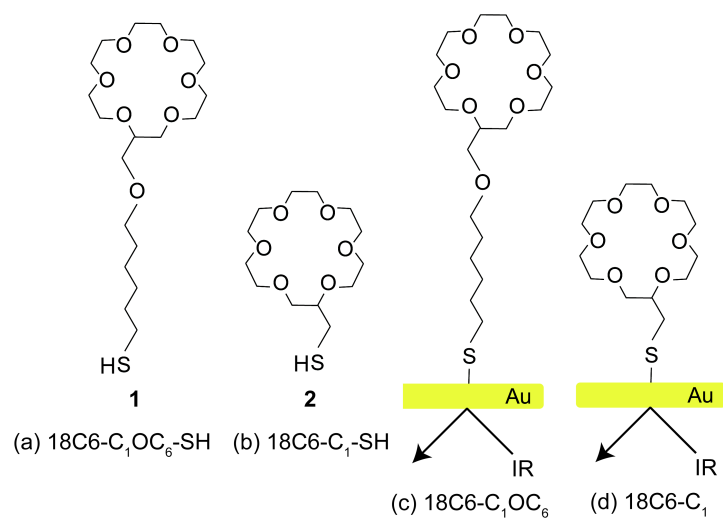


Figure 1. The structure of the crown ethers synthesized and chemisorbed on the gold surface.

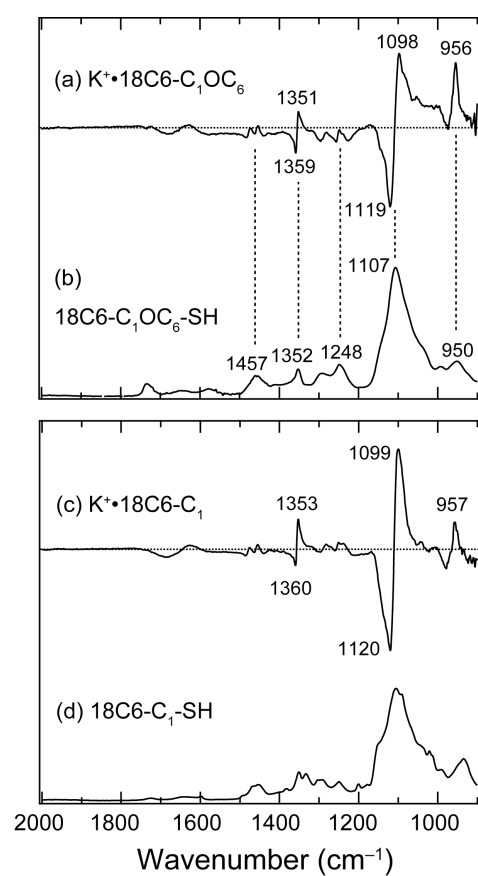


Figure 2. (a) The IR difference spectrum of the K⁺•18C6-C₁OC₆ complex on the gold surface with an aqueous solution of K⁺ (0.1 M). (b) The IR spectrum of 18C6-C₁OC₆-SH measured with an ATR FTIR spectrometer. (c) The IR difference spectrum of the K⁺•18C6-C₁ complex on the gold surface with an aqueous solution of K⁺ (0.1 M). (d) The IR spectrum of 18C6-C₁-SH measured with an ATR FTIR spectrometer.

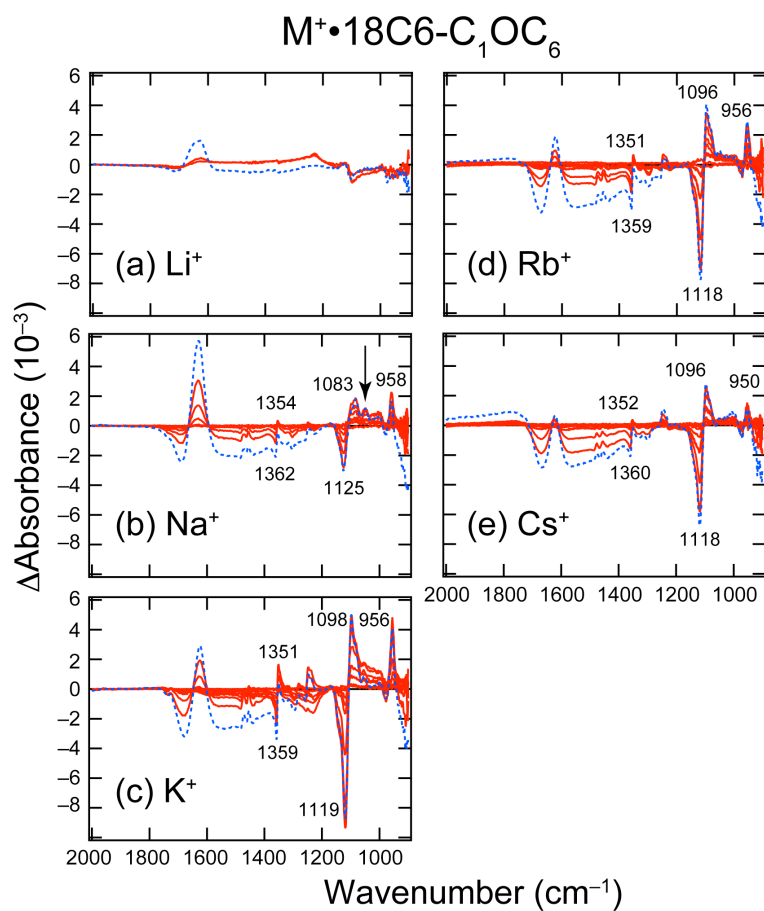


Figure 3. The IR difference spectra of the $M^+ \cdot 18C6-C_1OC_6$ ($M = Li, Na, K, Rb,$ and Cs) complexes on the gold surface. The concentration of the MCl salts ranges from 10^{-6} to 2 M. The dotted (blue) curves are the IR difference spectra measured at a salt concentration of 2 M.

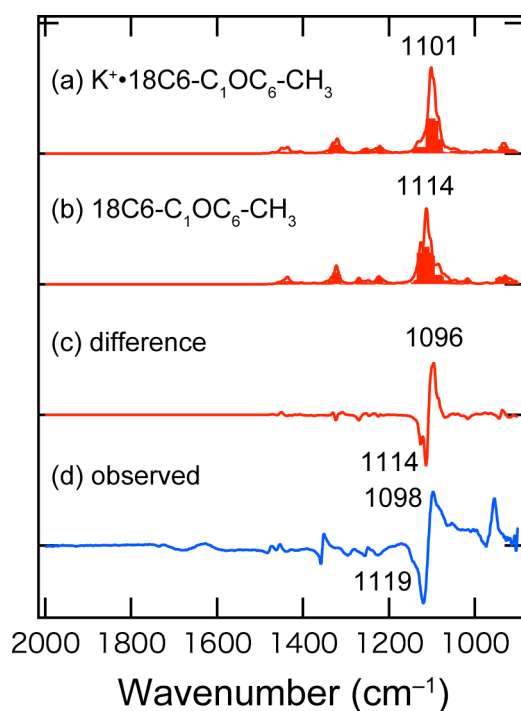


Figure 4. (a, b) The IR spectra of the $K^+ \cdot 18C6-C_1OC_6-CH_3$ complex and bare $18C6-C_1OC_6-CH_3$ calculated at the M05-2X/6-31+G(d) level with the PCM of water. A scaling factor of 0.9389 is employed for the calculated vibrational frequencies. The solid curves are the IR spectra reproduced by providing a Lorentzian component with a FWHM of 10 cm⁻¹ to each vibration. (c) The IR difference spectrum made by subtracting the simulated IR spectrum of bare $18C6-C_1OC_6-CH_3$ in Fig. 4b from that of the $K^+ \cdot 18C6-C_1OC_6-CH_3$ complex in Fig. 4a. (d) The observed IR difference spectrum of the $K^+ \cdot 18C6-C_1OC_6$ complex on the gold surface with a K^+ concentration of 0.1 M.

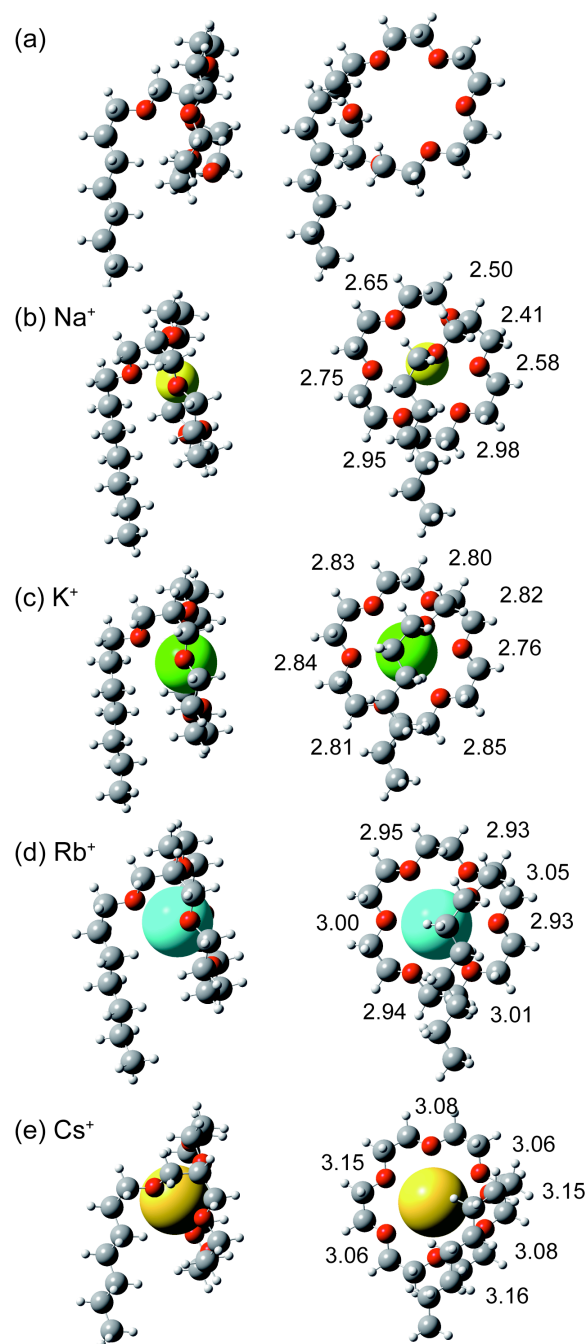


Figure 5. The calculated structure of bare 18C6-C₁OC₆-CH₃ and the M⁺•18C6-C₁OC₆-CH₃ (M = Na, K, Rb, and Cs) complexes. The numbers show the distance (Å) between the metal ion–oxygen atoms.

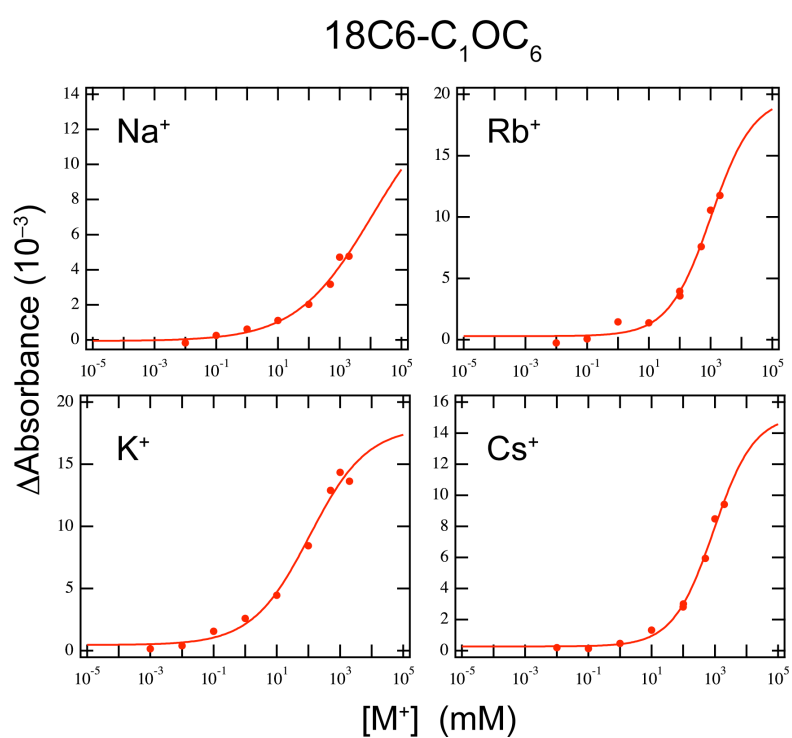


Figure 6. The peak-to-peak amplitude around 1100 cm^{-1} in the IR difference spectra of the $M^+ \cdot 18C6-C_1OC_6$ ($M = Na, K, Rb,$ and Cs) complexes (Fig. 3) as a function of the concentration of the M^+ ions (closed circles). The data are reproduced by Hill equations (solid curves).

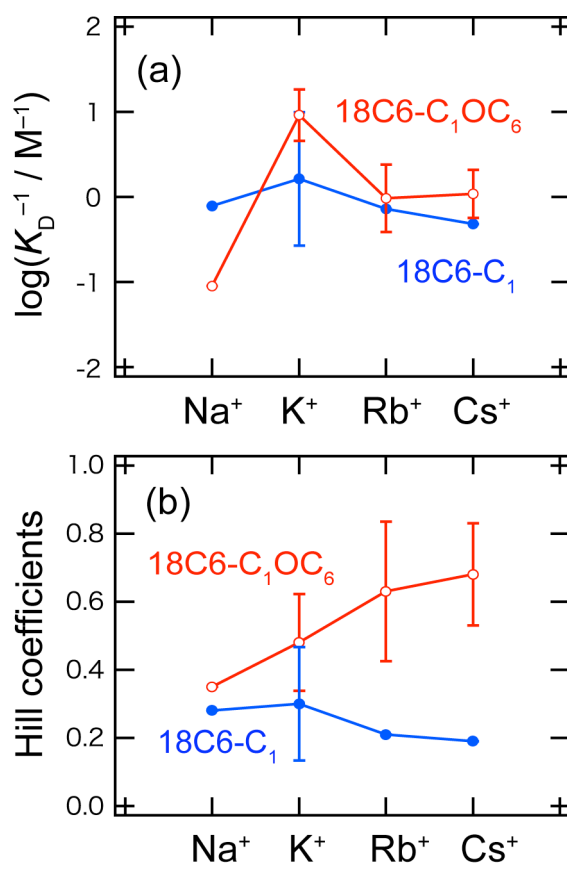


Figure 7. The reciprocal of the apparent K_D values and the Hill coefficients determined by fitting of the peak-to-peak intensity around 1100 cm^{-1} in the IR difference spectra of the $M^+ \cdot 18C6-C_1OC_6$ (red open circles) and $M^+ \cdot 18C6-C_1$ (blue closed circles) complexes.

References

- (1) Izatt, R. M.; Bradshaw, J. S.; Nielsen, S. A.; Lamb, J. D.; Christensen, J. J. *Chem. Rev.* **1985**, *85*, 271.
- (2) Izatt, R. M.; Terry, R. E.; Haymore, B. L.; Hansen, L. D.; Dalley, N. K.; Avondet, A. G.; Christensen, J. J. *J. Am. Chem. Soc.* **1976**, *98*, 7620.
- (3) Allen, F. H. *Acta Crystallogr. Sect. B-Struct. Commun.* **2002**, *58*, 380.
- (4) More, M. B.; Ray, D.; Armentrout, P. B. *J. Am. Chem. Soc.* **1998**, *121*, 417.
- (5) Hay, B. P.; Rustad, J. R.; Hostetler, C. J. *J. Am. Chem. Soc.* **1993**, *115*, 11158.
- (6) Dang, L. X. *J. Am. Chem. Soc.* **1995**, *117*, 6954.
- (7) Glendening, E. D.; Feller, D.; Thompson, M. A. *J. Am. Chem. Soc.* **1994**, *116*, 10657.
- (8) Inokuchi, Y.; Boyarkin, O. V.; Kusaka, R.; Haino, T.; Ebata, T.; Rizzo, T. R. *J. Am. Chem. Soc.* **2011**, *133*, 12256.
- (9) Inokuchi, Y.; Boyarkin, O. V.; Kusaka, R.; Haino, T.; Ebata, T.; Rizzo, T. R. *J. Phys. Chem. A* **2012**, *116*, 4057.
- (10) Inokuchi, Y.; Kusaka, R.; Ebata, T.; Boyarkin, O. V.; Rizzo, T. R. *ChemPhysChem* **2013**, *14*, 649.
- (11) Martinez-Haya, B.; Hurtado, P.; Hortal, A. R.; Hamad, S.; Steill, J. D.; Oomens, J. *J. Phys. Chem. A* **2010**, *114*, 7048.
- (12) Rodriguez, J. D.; Vaden, T. D.; Lisy, J. M. *J. Am. Chem. Soc.* **2009**, *131*, 17277.
- (13) Rodriguez, J. D.; Lisy, J. M. *J. Am. Chem. Soc.* **2011**, *133*, 11136.
- (14) Choi, C. M.; Kim, H. J.; Lee, J. H.; Shin, W. J.; Yoon, T. O.; Kim, N. J.; Heo, J. *J. Phys. Chem. A* **2009**, *113*, 8343.
- (15) Buchanan, G. W. *Prog. Nucl. Magn. Reson. Spectrosc.* **1999**, *34*, 327.
- (16) Antonio, M. R.; Dietz, M. L.; Jensen, M. P.; Soderholm, L.; Horwitz, E. P. *Inorg. Chim. Acta* **1997**, *255*, 13.
- (17) Ataka, K.; Giess, F.; Knoll, W.; Naumann, R.; Haber-Pohlmeier, S.; Richter, B.; Heberle, J. *J. Am. Chem. Soc.* **2004**, *126*, 16199.
- (18) Furutani, Y.; Shimizu, H.; Asai, Y.; Fukuda, T.; Oiki, S.; Kandori, H. *Journal of Physical Chemistry Letters* **2012**, *3*, 3806.
- (19) Osawa, M. *Bull. Chem. Soc. Jpn.* **1997**, *70*, 2861.
- (20) Flink, S.; Boukamp, B. A.; van den Berg, A.; van Veggel, F.; Reinhoudt, D. N. *J. Am. Chem. Soc.* **1998**, *120*, 4652.
- (21) Flink, S.; Schonherr, H.; Vancso, G. J.; Geurts, F. A. J.; van Leerdam, K. G. C.; van Veggel, F.; Reinhoudt, D. N. *J. Chem. Soc.-Perkin Trans. 2* **2000**, 2141.
- (22) Flink, S.; van Veggel, F.; Reinhoudt, D. N. *J Phys Chem B* **1999**, *103*, 6515.
- (23) Patel, G.; Kumar, A.; Pal, U.; Menon, S. *Chem. Commun.* **2009**, 1849.
- (24) Guo, H.; Kimura, T.; Furutani, Y. *Chem Phys* **2013**, *419*, 8.

(25) Mohamadi, F.; Richards, N. G. J.; Guida, W. C.; Liskamp, R.; Lipton, M.; Caufield, C.; Chang, G.; Hendrickson, T.; Still, W. C. *Journal of Computational Chemistry* **1990**, *11*, 440.

(26) Frisch, M. J.; Trucks, G. W.; Schlegel, H. B.; Scuseria, G. E.; Robb, M. A.; Cheeseman, J. R.; Scalmani, G.; Barone, V.; Mennucci, B.; Petersson, G. A.; Nakatsuji, H.; Caricato, M.; Li, X.; Hratchian, H. P.; Izmaylov, A. F.; Bloino, J.; Zheng, G.; Sonnenberg, J. L.; Hada, M.; Ehara, M.; Toyota, K.; Fukuda, R.; Hasegawa, J.; Ishida, M.; Nakajima, T.; Honda, Y.; Kitao, O.; Nakai, H.; Vreven, T.; Montgomery, J., J. A.; Peralta, J. E.; Ogliaro, F.; Bearpark, M.; Heyd, J. J.; Brothers, E.; Kudin, K. N.; Staroverov, V. N.; Kobayashi, R.; Normand, J.; Raghavachari, K.; Rendell, A.; Burant, J. C.; Iyengar, S. S.; Tomasi, J.; Cossi, M.; Rega, N.; Millam, N. J.; Klene, M.; Knox, J. E.; Cross, J. B.; Bakken, V.; Adamo, C.; Jaramillo, J.; Gomperts, R.; Stratmann, R. E.; Yazyev, O.; Austin, A. J.; Cammi, R.; Pomelli, C.; Ochterski, J. W.; Martin, R. L.; Morokuma, K.; Zakrzewski, V. G.; Voth, G. A.; Salvador, P.; Dannenberg, J. J.; Dapprich, S.; Daniels, A. D.; Farkas, Ö.; Foresman, J. B.; Ortiz, J. V.; Cioslowski, J.; Fox, D. J. In *Gaussian 09, Revision A.1*; Gaussian, Inc.: Wallingford CT, 2009.